



Effect of Upper Tropospheric Vertical Thermal Contrast Over the Mediterranean Region on Convection over the Western Tibetan Plateau during ENSO Years

B. H. Vaid & X. San Liang

To cite this article: B. H. Vaid & X. San Liang (2020) Effect of Upper Tropospheric Vertical Thermal Contrast Over the Mediterranean Region on Convection over the Western Tibetan Plateau during ENSO Years, Atmosphere-Ocean, 58:2, 98-109, DOI: [10.1080/07055900.2020.1751048](https://doi.org/10.1080/07055900.2020.1751048)

To link to this article: <https://doi.org/10.1080/07055900.2020.1751048>



Published online: 16 Jun 2020.



Submit your article to this journal [↗](#)



Article views: 28



View related articles [↗](#)



View Crossmark data [↗](#)

Effect of Upper Tropospheric Vertical Thermal Contrast Over the Mediterranean Region on Convection over the Western Tibetan Plateau during ENSO Years

B. H. Vaid * and X. San Liang

School of Marine Sciences, Nanjing University of Information Science and Technology (NUIST), Nanjing, People's Republic of China

[Original manuscript received 3 June 2019; accepted 14 February 2020]

ABSTRACT *Using the National Centers for Environmental Prediction–Department of Energy Atmospheric Model Intercomparison Project 2 daily reanalysis datasets, the present study reveals that an upper tropospheric vertical thermal contrast (VTC) exists between pressure levels at 100 and 250 hPa over the Mediterranean region (MR) during the midsummer monsoon. An increase and decrease in the tropospheric temperature (TT) at the 100 and 250 hPa levels respectively, are found to be centred over the MR during El Niño years. The former is characterized by an anticyclonic circulation in the wind shear and the latter by a cyclonic circulation. The opposite pattern is exhibited during La Niña years. It is shown that the MR VTC remotely affects convection over the western Tibetan Plateau (WTP) by inducing favourable temperature, circulation patterns, and ascending (descending) winds on the upper vertical levels of the WTP during El Niño (La Niña) years. This effect has been further substantiated by a careful causality analysis with a new causal inference technique, which identifies a dominant causality from the MR VTC to the WTP longwave fluxes through the top of the atmosphere.*

RÉSUMÉ *[Traduit par la rédaction] En utilisant les données de réanalyse quotidiennes du projet 2 d'intercomparaison des modèles atmosphériques du National Centers for Environmental Prediction du Department of Energy des États-Unis, cette étude révèle qu'un contraste thermique vertical existe dans la haute troposphère entre les niveaux de pression 100 hPa et 250 hPa, sur la région de la Méditerranée, pendant la mousson de la mi-été. Une augmentation et une diminution de la température troposphérique aux niveaux 100 hPa et 250 hPa, respectivement, sont centrées sur la région en question pendant les années El Niño. L'augmentation est caractérisée par une circulation anticyclonique dans le cisaillement du vent et la diminution, par une circulation cyclonique. La situation s'inverse pendant les années La Niña. Il est démontré que le contraste thermique vertical au-dessus de la Méditerranée influe à distance sur la convection se formant sur le plateau tibétain occidental, en induisant des températures, une circulation et des vents ascendants (descendants) favorables en altitude au-dessus de cette partie du plateau, pendant les années El Niño (La Niña). Cet effet a été corroboré par une analyse minutieuse de la causalité à l'aide d'une nouvelle technique d'inférence, qui détermine la relation de cause à effet dominante entre le contraste thermique au-dessus de la Méditerranée et les flux d'ondes longues du plateau tibétain occidental à travers le sommet de l'atmosphère.*

KEYWORDS upper tropospheric temperature (TT); thermal contrast; midsummer monsoon; convection; causality analysis

1 Introduction

The Mediterranean region (MR) is situated in a transitional geographical zone bounded by the North African desert and the Euro-Asian region; it is often observed to be affected by continental and maritime air masses of completely different origins (Meteorological Office, 1962; Barry and Chorley, 2003). The geographic location and socio-economic conditions make the MR vulnerable to climate change. In fact, it has been identified as one of the regions most responsive to climate change around the world (Giorgi, 2006). As an

example, it is significantly affected by the El Niño–Southern Oscillation (ENSO; Alpert et al., 2005).

Considered to be the most prominent coupled air–sea interaction in the tropical Pacific, ENSO alternates between anomalously warm (El Niño) and cold (La Niña) sea surface temperature (SST) conditions (Bjerknes, 1969; Kessler, 2002). It remotely affects extreme weather events in various parts of the globe through atmospheric teleconnections (Yu and Zou, 2013; Ward et al., 2014; Chiodi and Harrison, 2015; Vaid and Liang, 2019). Previously, ENSO had been

*Corresponding author's email: bakshi32@gmail.com

considered to be irrelevant to the MR or only a marginal factor (Ropelewski and Halpert, 1987). Later it was found that a consistent ENSO signal exists in the region though the signal itself may be variable (e.g., Mathieu et al., 2004). For example, ENSO conditions give rise to pronounced anomaly patterns in seasonal climate in the MR as well (e.g., Alpert et al., 2005; Yu and Zou, 2013; Ward et al., 2014). Ehsan et al. (2013) found that ENSO affects the MR by contributing to the interannual variability of storm frequency and precipitation. The storms play the role of an atmospheric bridge through which the effects of the ENSO-related tropical Pacific SST anomalies are taken into the mid-latitudes (Abid et al., 2015). Note that the influence of ENSO on the region may be modified by other factors, such as large interannual variability of the atmospheric circulation over the Atlantic-European sector, which make the regional atmospheric dynamics subtle and might be nonstationary on multidecadal scales (Bronnimann, 2007). These significant relationships between ENSO and its remote effects form a solid basis for seasonal to longer time scale temperature predictions over the MR that have aroused widespread concern in the changing climate.

In the MR extreme temperature is a major concern, considering its potential impact on natural and human systems there. Beniston and Stephenson (2004) showed that an increase in temperature over the course of the twenty-first century is likely to produce an increase in the frequency of severe heatwave episodes in the MR. In addition, the surface of the MR has been continuously warmed during the last several decades, especially during midsummer (Brunetti et al., 2004; Volosciuk et al., 2016). In the future, it is projected that a 2°C increase in global mean temperature implies a 3°C warming in hot temperature extremes in the MR (Seneviratne et al., 2016). Depending on the climate trend (Stocker et al., 2013), a rise in temperature from 2° to 6°C by 2100 is expected in the MR, making it an important region for study in the context of ecosystems and human well-being and explicitly attracts a wide range of international academic attention regarding global changes.

Considering the importance of the MR, several attempts have been made to understand the temperature variation over the MR, which is associated with widespread synoptic systems and also human health concerns (Saaroni et al., 2003; Xoplaki et al., 2004; Tolika et al., 2009), but these are mostly limited to lower level temperature variation. However, it is known that most climate change processes occur in the upper troposphere as well, so the upper tropospheric temperature (TT) variation should also be taken into account in evaluating climate variability. Recently, temperature changes in the upper troposphere have attracted increasing attention because of their connection to precipitation variation, large-scale circulation, and surface climate variability on a wide range of time scales (Liu and Yanai, 2001; Zhou and Zhao, 2010; Zuo et al., 2012). But, as one of the important signals characterizing climate change, the study of the TT is still far from sufficient, particularly for the MR. This study intends to close that gap. Specifically, we want to examine

variations in the upper TT in midsummer (i.e., July–August) over the MR and its associated impacts.

In comprehending the TT variation over the MR, it was found to be remotely impacted by convective systems over central and eastern Europe and the surrounding basin area (Lionello et al., 2006; Sodemann and Zubler, 2010; Ciric et al., 2018). But, to the best of our knowledge, there has not been any study of its relation to convective systems over the western Tibetan Plateau (WTP), a region that, during mid-monsoon months, has been shown to be the most important heat source region in East Asia (Xu et al., 2008; Ma et al., 2017; Vaid and Liang, 2018a, 2018b). The Tibetan Plateau (TP) has been recognized as the water tower of Asia (Immerzeel et al., 2010) and is well known for its profound importance to regional and global climate through dynamical and thermodynamical processes (Wu et al., 2015; Bao et al., 2010). For example, Kitoh (2004) found that the Mei-Yu-Baiu rainfall intensifies and extends to inland Asia with increasing TP uplift. Wang et al. (2008) suggested that the heating induced by increasing temperature over the TP could enhance East Asian summer rainfall, suggesting that rising TP temperature in the near future may result in further strengthened summer rainfall over East Asia. Wu et al. (2012b) showed that the TP heat source and sink and snow cover and depth modulate the effect of ENSO on the Asian summer monsoon. In addition, in the summer the TP can also be responsible for the northern China heatwave frequency on decadal-to-interdecadal time scales (Wu et al., 2012a); the TP can affect (Abe et al., 2013) the onset of the South Asian monsoon by modulating the air–sea interaction in the Indian Ocean. Recently, summer heatwave frequency in southern Europe and northeastern Asia has been linked to anomalous summer snow cover on the TP (Wu et al., 2016). For these reasons, it has been shown that the TP atmospheric heat source and sink may act as a potential indicator for climate forecasts at shorter time scales (Orsolini et al., 2013; Senan et al., 2016; Lin et al., 2016). Because the TP is a water source for Asia's major rivers (Fekete et al., 1999, 2000), affecting the lives of one-quarter of the world's population, it is highly desirable to determine whether or not any teleconnection exists because this may lead to regional water cycle variabilities and extreme events, such as severe and extreme drought and flood. In this study we focus on the connection between the convective systems over the WTP and the MR. To the best of our knowledge, no study on this topic currently exists in the literature.

Hence, we specifically want to (i) examine the upper tropospheric vertical thermal variation over the MR during the midsummer monsoon and (ii) study the causes of the TT variation over the MR, in particular, the possible relation between the upper TT variation over the MR and that over the WTP during ENSO years. In Section 2, we introduce the data and analysis methods. Section 3 is devoted to examining the upper TT variation over the MR and its associated relationship with atmospheric convection over the WTP. Our study is summarized in Section 4.

JA Niño-3 index

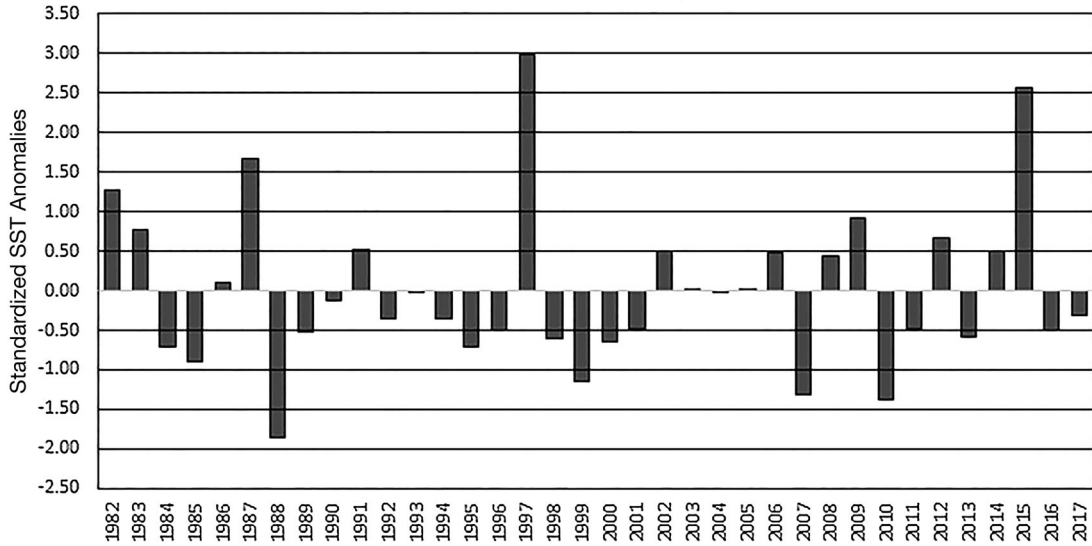


Fig. 1 Standardized JA SST anomalies based on the Niño-3 index.

2 Data and methodology

We derive the wind fields, air temperature, and geopotential height (Kanamitsu et al., 2002) from the National Centers for Environmental Prediction (NCEP)–Department of

Energy (DOE) Atmospheric Model Intercomparison Project 2 (AMIP 2) daily reanalysis datasets for the period 1982–2017 (NOAA, 2019a). For composite analysis the data during the midsummer monsoon (i.e., July and August for

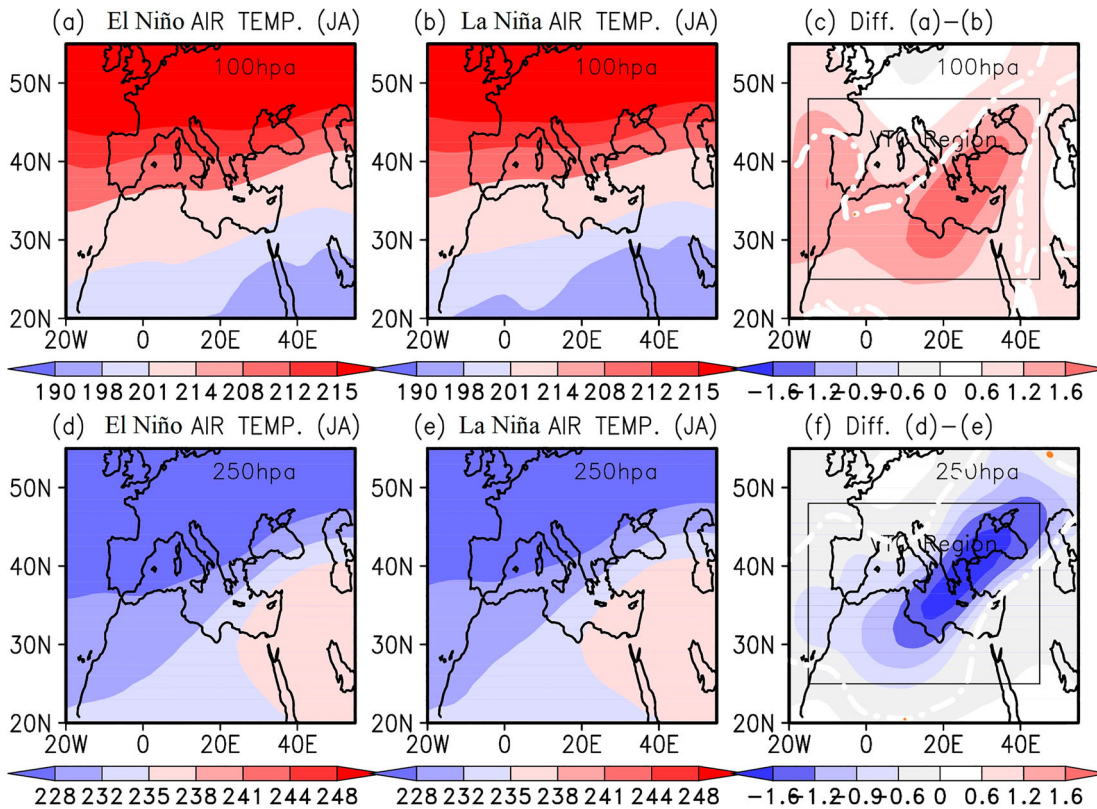


Fig. 2 JA TT (K) for the 100 hPa level during the (a) El Niño and (b) La Niña events. (c) The difference between (a) and (b) (i.e., (a)–(b)). In (c), the thick white dashed line indicates the areas statistically significant at the 99% level based on a Student’s *t*-test. (d) to (f) as in (a) to (c), but for the 250 hPa level.

the years from 1982 to 2017) are used. These two months (i.e., July and August) were chosen because the MR temperature reaches its maximum during that period (Alpert et al., 1990; Saaroni and Ziv, 2000; Saaroni et al., 2003), causing economic loss and human health problems. Other data include the long-wave flux (LWF), which are acquired from the Modern Era Retrospective-analysis for Research and Applications (MERRA; Rienecker et al., 2011), and the SST anomalies, which are derived from the National Oceanic and Atmospheric Administration (NOAA) Optimum Interpolation (OI) SST, v2 (OISSTV2), dataset (Reynolds et al., 2002; NOAA, 2019b). The ENSO events during the midsummer monsoon (JA) for the period 1982–2017 are identified using the SST anomaly-based Niño-3 index (area-averaged SST anomaly over 150°–90°W, 5°N–5°S). The index is normalized by its standard deviation, and the years with a standard deviation above 0.5 are considered an event year for the purposes of this study (more details can be found in Fig. 1). Based on the Niño-3 JA index for the 1982–2017 period (Fig. 1), the midsummer monsoon in the nine years, JA 1982, 1983, 1987, 1991, 1997, 2009, 2012, 2014, and 2015 are identified as El Niño mid-monsoon years, and eleven other mid-monsoon years (i.e., JA 1984, 1985, 1988, 1989, 1995, 1998, 1999, 2000, 2007, 2010, and 2013) are identified as La Niña years. In general, ENSO events are mainly represented by the Niño-3 index and Niño-3.4 index. We chose Niño-3 because it has been found to be the optimal index for monitoring El Niño compared with other Niño indices. In other words, all other Niño indices are found to be less efficient at distinguishing between El Niño and El Niño Modoki signals or are easily adulterated by El Niño Modoki signals (Li et al., 2010). Nonetheless, we also repeated the study using the Niño-3.4 index; as expected, the results do not make a significant difference. In this study, significance is mainly determined using a Student's *t*-test with 62 degrees of freedom.

To quantitatively examine the measurable impact of the upper TT thermal contrast on the atmospheric variables, for example, LWF, over the study region during the midsummer monsoon, we used a newly developed theory and methodology to rigorously identify the causality between time series (Liang, 2014, 2015, 2016, 2018). We adopted a

modified version of that methodology, the “composite causality analysis,” as detailed in Vaid and Liang (2019), for application in this study. In the following we provide a brief description.

Causality analysis is one of the most important topics lying at the heart of scientific research. During the past few years, Liang (2014, 2016) established that the causality between two series, say, X_1 and X_2 , can be rigorously derived from first principles; it can also be quantitatively evaluated. (For a one-page review of the theory the reader is referred to Section 2 of Liang (2018)). The resulting formula is very concise in form and very easy to use. In the linear limit, the maximum likelihood estimator (MLE) of the causality from X_2 to X_1 (nats per unit time) is

$$T_{2 \rightarrow 1} = \frac{C_{11}C_{12}C_{2,d1} - C_{12}^2C_{1,d1}}{C_{11}^2C_{22} - C_{11}C_{12}^2}, \quad (1)$$

where C_{ij} is the sample covariance between the two time series X_i and X_j ($i, j = 1, 2$), and $C_{i,dj}$ is the covariance between X_i and a derived series

$$\dot{X}_j = \frac{X_j(t + k\Delta t) - X_j(t)}{k\Delta t},$$

that is, a series formed from $X_j(t)$ through taking Euler forward differencing, with Δt being the time step and $k \geq 1$ some integer. (Note this is the MLE of the rigorously derived causality in the linear case; for the original non-linear formula, see Liang (2016).) Ideally, when $T_{2 \rightarrow 1}$ is non-zero, then X_2 is causal to X_1 , otherwise it is not causal. In practice, statistical significance must be tested (Liang, 2015) before reaching a conclusion as to whether a causality exists or not. In the present study, the computed causality is at the 95% confidence level.

Composite causality analysis is a causality analysis in combination with composite analysis. As detailed in Vaid and Liang (2019), first the causalities are computed using Eq. (1) on running time windows (i.e., form a “field of causality”) at all the time steps. For a time series of length N (with time steps 1, 2, 3, ..., N), suppose we consider a time window of

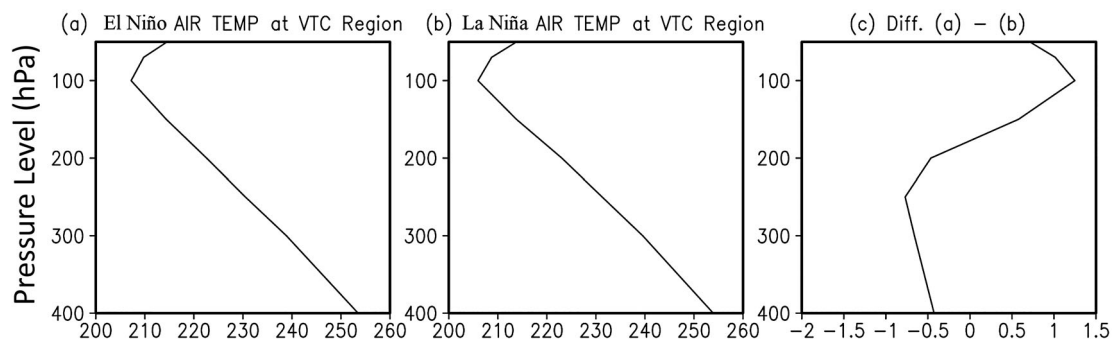


Fig. 3 Vertical variation of JA air temperature over the VTC region during (a) El Niño and (b) La Niña events. (c) The difference between (a) and (b) (i.e., (a)–(b)). The difference between (a) and (b) is statistically significant at the 99% level based on a Student's *t*-test.

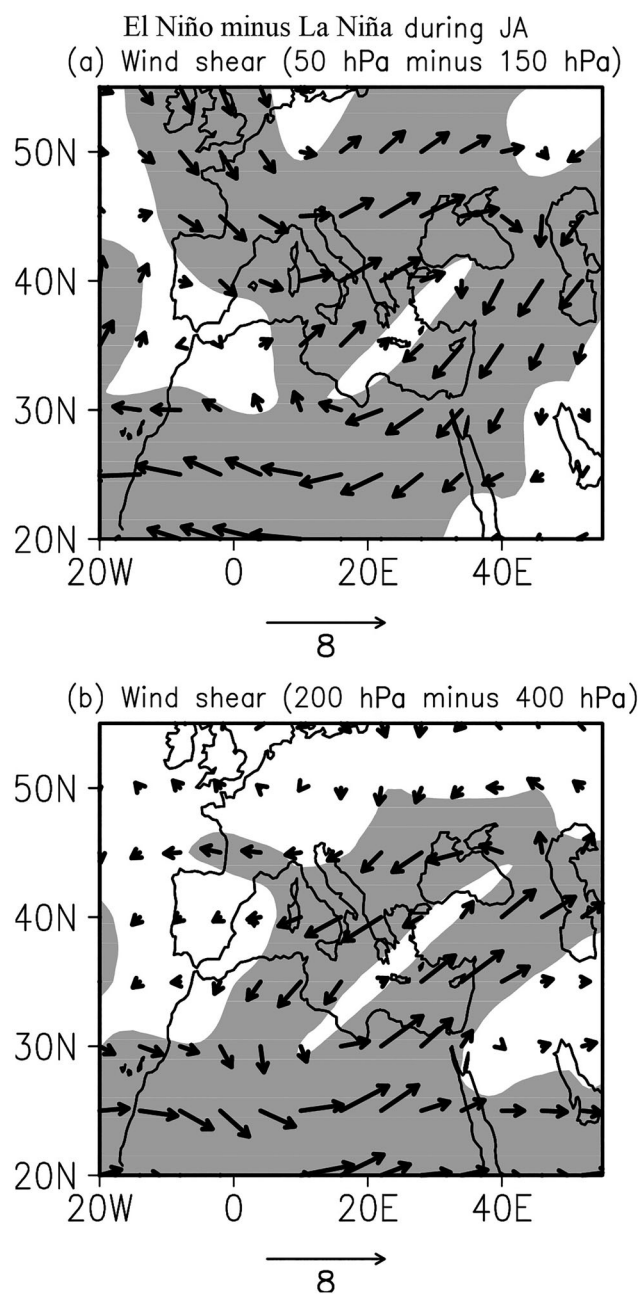


Fig. 4 JA wind shear (m s^{-1}) (El Niño minus La Niña events): (a) 50 hPa–150 hPa and (b) 200 hPa–400 hPa. The shaded region is statistically significant at the 99% level based on a Student's t -test.

length M , with $M < N$. We first perform the analysis for the sub-series at steps 1, 2, ..., M , then slide the window to the right by 1 and carry out the analysis for the sub-series on steps 2, 3, ..., $M+1$, and so forth. In the end, we will obtain a series of causality on time steps centred at these sliding windows (no value for the beginning $M/2$ steps and the last $M/2$ steps). Once this is done, these causalities can be composited based on some criterion (e.g., the criterion to pick out El Niño events). In this way the composite causalities for the El Niño and La Niña events are obtained.

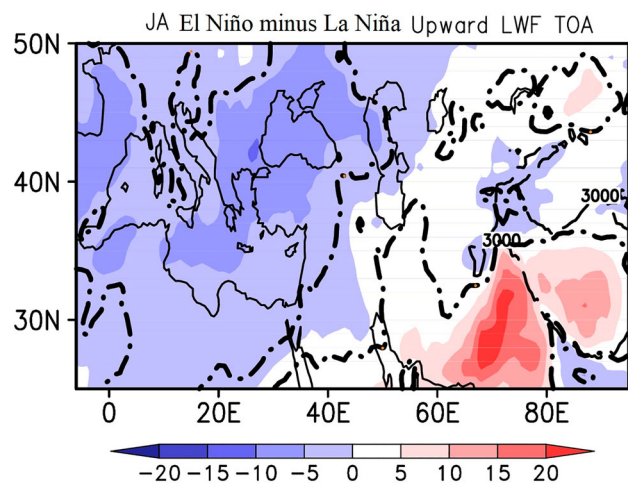


Fig. 5 JA LWF top of the atmosphere TOA (W m^{-2}) (El Niño minus La Niña events). The dashed line marks the 3000 m topographic isoline. The enclosed region marked by the thick black contour (dot-dashed line) is statistically significant at the 99% level based on a Student's t -test.

As a supplement, traditional analyses (e.g., regression analysis) are also used to explore the potential relationships between the upper TT variation over the MR and large-scale atmospheric circulation patterns over the WTP.

3 Results

We mainly examine the upper TT variation (i.e., between pressure levels 400 hPa and 50 hPa) over the MR during the mid-monsoon months. We are particularly interested in the 250 hPa and 100 hPa levels because the TT at these levels is found to be most variable. Figure 2 shows the July–August (JA) averaged TT for El Niño (Figs 2a and 2d) and La Niña (Figs 2b and 2e) periods for the 100 and 250 hPa levels, respectively. The difference and associated confidence level (shaded with white contours) are displayed in Figs 2c and 2f. To check the statistical significance of the difference as observed, a Student's t -test was performed. It can be seen that the 100 hPa TT and the 250 hPa TT have undergone substantial changes. Interestingly, the difference between the TTs during the El Niño and La Niña periods is organized into a strong vertical thermal contrast centred over the MR (15°W – 45°E , 25°N – 48°N ; hereafter VTC region). Figures 2c and 2f show TT differences (i.e. the TT during the El Niño events minus that during the La Niña events). Figure 2c exhibits an obvious dipole pattern during El Niño events with a positive pattern at 100 hPa, while at 250 hPa, it reveals a negative pattern (Fig. 2f). The troposphere at 100 hPa seems to be much warmer during El Niño events than during La Niña events, whereas at 250 hPa it is cooler. Interestingly, the warming and cooling of the TT is confined within the VTC region in the two ENSO phases. We have also explored the connection without the influence of ENSO. The difference between the air temperature patterns for neutral and ENSO years (figure not shown) reveals no such VTC over the MR.

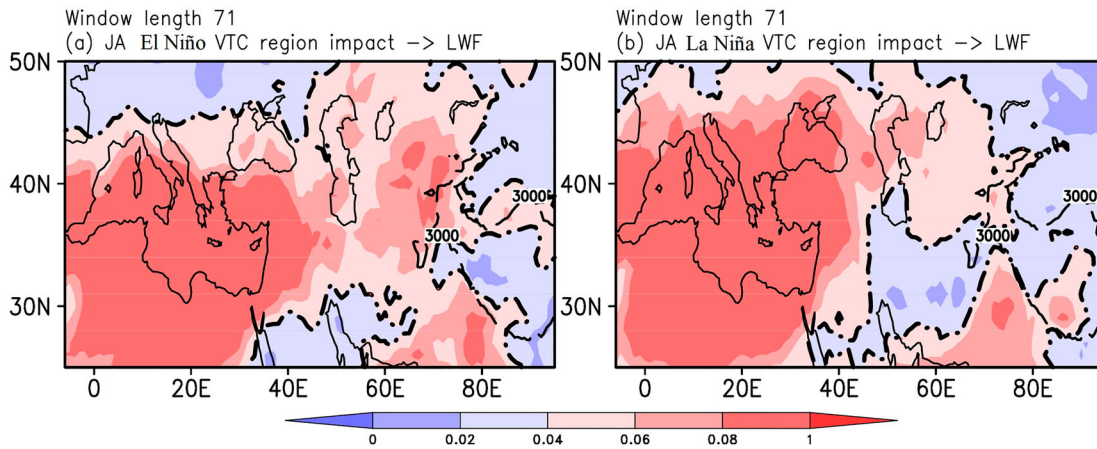


Fig. 6 The causality (information flow in nats d^{-1}) from the VTC region to the LWF at TOA, for a time window size of 71 days: (a) JA El Niño events and (b) JA La Niña events. Nat is the unit for entropy, which has the form of $\int \rho \log \rho$ (ρ being the probability density function) when the logarithm uses base e. The dashed line marks the 3000 m topographic isoline. The causality enclosed in the thick black contour (dot-dashed line) is at the 95% confidence level.

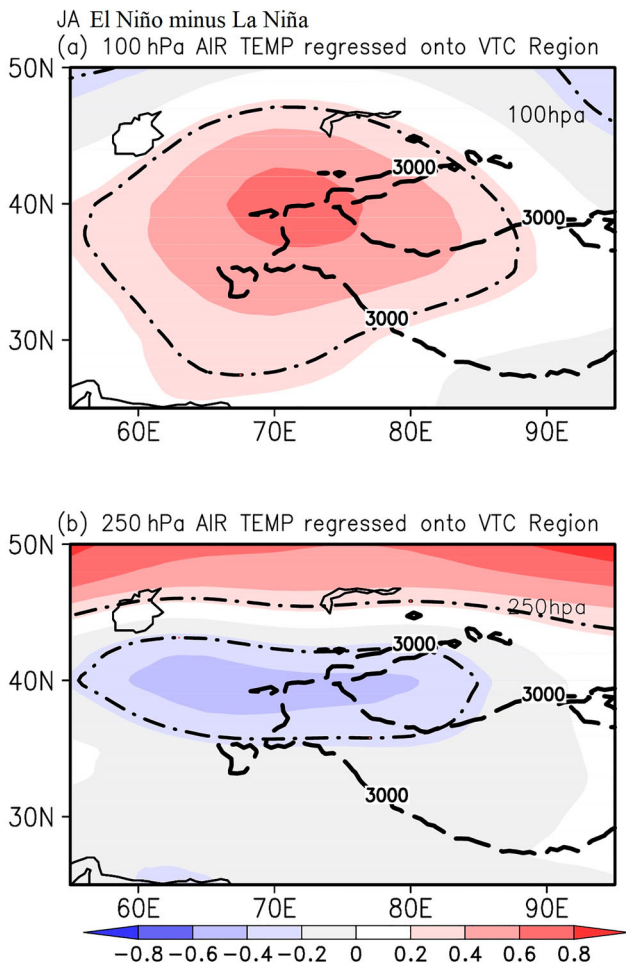


Fig. 7 (a) Air temperature (K) at 100 hPa regressed onto the VTC for El Niño minus La Niña events. (b) As in (a) but for 250 hPa. The regression coefficients (thick dot-dashed black contours) are statistically significant at the 99% level. Shown are regressed air temperature on a $1^\circ \times 1^\circ$ latitude–longitude grid. The dashed line marks the 3000 m topographic isoline.

This study is about the effect of upper tropospheric VTC over the MR on the convection over the western TP during ENSO years, so we leave the study of El Niño’s influence on the upper tropospheric VTC over the MR to future studies.

To examine the thermal contrast occurring in the upper troposphere over the VTC region in more detail, the vertical profiles of average air temperature during the midsummer monsoon are plotted. Shown in Figs 3a and 3b are the profiles for El Niño and La Niña periods, respectively, and the difference between them (Fig. 3c). A closer look at the difference (Fig. 3c) reveals that a sharp VTC in the TT exists over the VTC region, with one pole at 100 hPa and another over 250 hPa. Hence, we define it as VTC over the MR because the difference between the TTs exists over these centres (i.e., differences between 250 hPa and 100 hPa; hereafter VTC). Previous studies have shown that the TT variations play a vital role in convection changes during the monsoon season (Vaid and Liang, 2015; 2018a; 2018b; 2019), so we speculate that this strong VTC in the VTC region during El Niño and La Niña events may cause a measurable impact on convection over the MR and surrounding regions, which we now explore.

Considering the relation between thermal contrast and convection, the observed variation above will inevitably exert an influence on the local climate in the context of mid-monsoon variation over the MR and the surrounding area. In the following we first look at how the upper tropospheric circulation may change during ENSO. For this purpose, we compute the wind shear vectors around the 100 and 250 hPa levels by subtracting the wind vectors at 150 hPa from those at 50 hPa, and subtracting those at 400 hPa from those at 200 hPa. We then take their respective averages over the El Niño and La Niña periods and subtract the former from the latter. The resulting difference field is drawn in Figs 4a and 4b. Clearly, the results are well correlated with the TT difference pattern (Figs 2c and 2f). In particular, the closed loop circulation structures are clearly seen over the MR. In the upper layers at 100 hPa the circulation is anticyclonic and at 250 hPa it is cyclonic (Figs

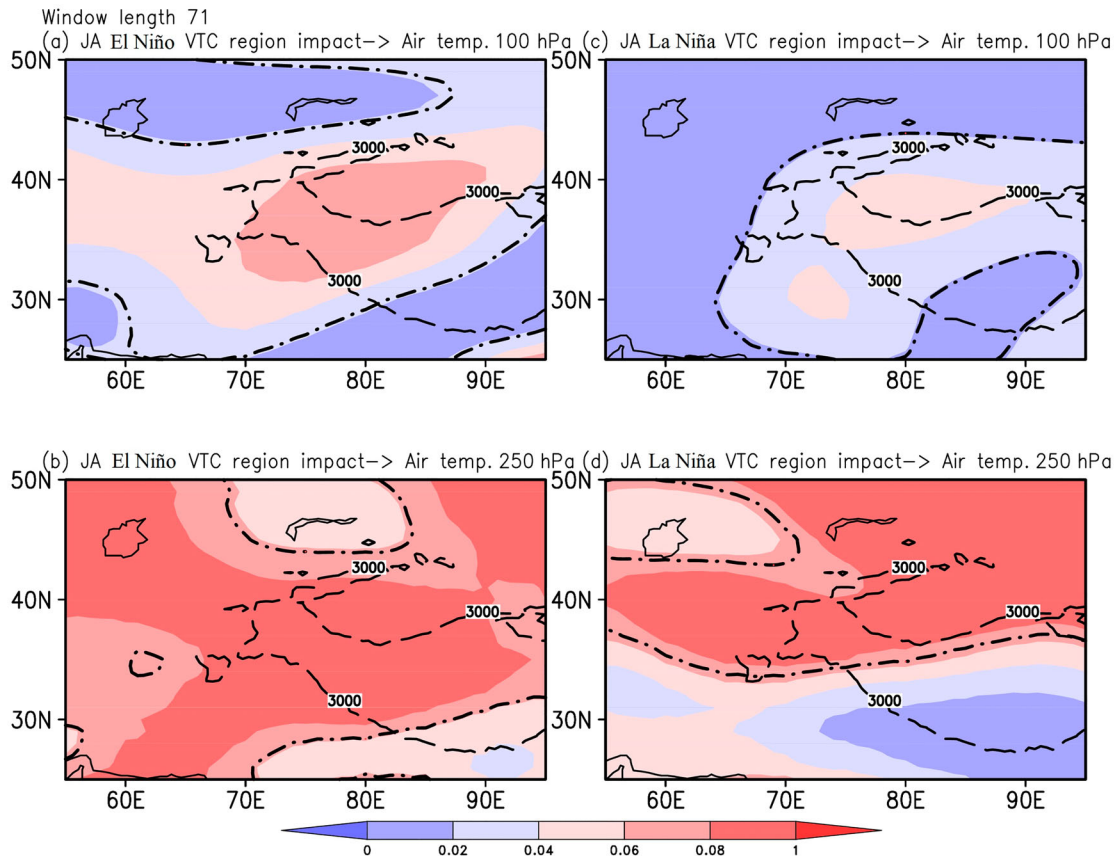


Fig. 8 The causality (information flow nats d^{-1}) from the VTC region to the air temperature at the 100 hPa level for a time window size of 71 days: (a) JA El Niño events and (c) JA La Niña events. (b) and (d) as in (a) and (c) but for the 250 hPa level. The dashed line marks the 3000 m topographic isoline. The causality enclosed in the thick black contour (dot-dashed line) is at the 95% confidence level.

4a and 4b, respectively) during El Niño, while during La Niña events the opposite circulation pattern appears (figure not shown). According to the ideal gas law, we know that pressure multiplied by the specific volume equals the temperature multiplied by a constant, which implies that, given specific volume, temperature decreases as air pressure decreases. Thus, the associated causes of the VTC over the MR can be seen in the upper troposphere circulation changes during ENSO years (Fig. 4). Because cyclonic circulation leads to ascending winds, which are considered a sign of convection (Vaid and Liang, 2018a); it is, therefore, possible that, associated with the TT change and aforementioned system, there is an increase (decrease) in convection in the MR and surrounding regions during El Niño (La Niña) years. The LWF in ENSO during the midsummer monsoon period also exhibits consistent variations. In Fig. 5 we plot the surplus (El Niño minus La Niña) upward LWF through the top of the atmosphere. We see a clear increase in LWF, in agreement with the TT variation (Figs 2c and 2f) and wind variation as observed above (Figs 4a and 4b).

To examine the direct relationship between the TT variation over the MR and LWF we use the time series of a VTC (as defined above) over the MR, then apply to it and the series of LWF, a newly developed composite causality analysis,

which is detailed in the appendix of Vaid and Liang (2019). We tried different sizes of time windows, such as 41, 51, 61, and 71 days, and the resulting causal patterns are similar. The results are shown in Fig. 6. As can be seen, the VTC over the MR is causal to the LWF. It is worth noting that the causalities obtained here are asymmetric in direction; that is to say, they are from the VTC over the MR to convection over the region and its surrounding area, and it is not the other way around (i.e., not from the LWF to VTC). This is in contrast to traditional tools, such as correlation analysis, which is symmetric and, hence, cannot determine what causes what. Besides, we have not only been able to determine the directions of causality but also the magnitudes.

A closer look at Fig. 5 shows that, along with the increase in the convection over the MR, there is also a similar convection pattern over the WTP. We postulate that it may have something to do with the MR VTC. To determine whether this is true or not, it is interesting to note that the resulting causalities above show that the impact of the MR VTC is not only limited to within the MR only but can also be extended to the WTP (Fig. 6). In fact, a large impact on convection over the WTP during El Niño and La Niña events is clearly seen. We know that the TP is the highest plateau in the world, with an average altitude over 3000 m, and has a significant effect on

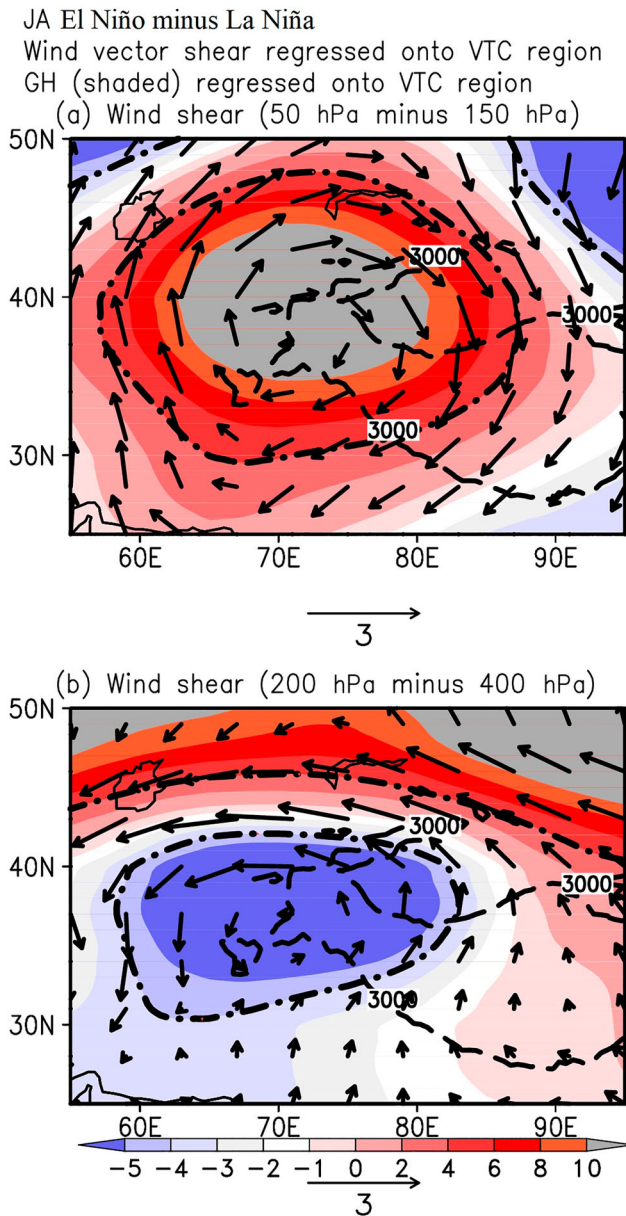


Fig. 9 JA wind shear (m s^{-1}) (El Niño minus La Niña events) and geopotential height (shaded, m) regressed onto VTC: (a) 50 hPa–150 hPa; (b) 200 hPa–400 hPa. The regression coefficients enclosed by the thick black dot-dashed line are statistically significant at the 99% confidence level. The regressed wind vectors and geopotential height are shown on a $1^\circ \times 1^\circ$ latitude–longitude grid. The dashed line marks the 3000 m topographic isoline.

the climate and environmental processes over Asia (e.g., Ye and Gao, 1979; Vaid and Liang, 2018a, 2018b). This noteworthy result is of scientific importance. We also know that the TP is prone to devastating threats (e.g., abundant rainfall, flooding episodes, and landslides) during the midsummer monsoon, but the reason has been poorly understood. The foregoing result indicates that the MR VTC could be a remote driver because it may modulate the WTP circulation and, hence, the upper TT, thereby, influencing the convection over the WTP.

To better understand the relationship between the MR VTC and convection over the WTP as specified in Figs 5 and 6, the upper TT over the WTP is regressed onto the VTC over the MR. Interestingly, the VTC is seen to induce a thermal contrast between the 100 and 250 hPa levels over the WTP region with positive (negative) temperature anomalies over the 100 (250) hPa level; that is to say, the VTC seems to be responsible for inducing favourable conditions for convection over the WTP (Figs 7a and 7b). The induced vertical temperature dipole structure between the upper troposphere (centred at 250 hPa) and the lower stratosphere (centred at 100 hPa) suggests the role of the MR in inducing the aforementioned opposing temperature changes. To further corroborate the assertion about the role of VTC over the MR on the WTP, we chose to perform composite causality to examine the cause and effect of the MR VTC. Interestingly, the computed causality clearly exhibits the cause and effect between the MR VTC and the air temperature over the WNP (Fig. 8). In particular, the MR VTC is found to be causal to the air temperature over the WTP, substantiating our finding that the VTC seems to be responsible for convection over the WTP.

The aforementioned induced TT pattern (Fig. 7) can be understood through analyzing the wind shear field regressed (c.f. Figs 4a and 4b for more details regarding the chosen wind shear vectors) onto the MR VTC (Fig. 9). As shown in Figs 9a and 9b, the El Niño minus La Niña VTC seems to be concomitant with the induced 100 and 250 hPa TT variation (Fig. 7), with a noticeable anticyclonic and cyclonic circulation in the wind shear positioned over the WTP, respectively, whereas the La Niña minus El Niño VTC circulation is more or less mirrored there (figure not shown because it is simply the opposite of Figs 9a and 9b). The geopotential height distribution also supports this (Fig. 9, shading).

The structure in Fig. 9 implies increasing ascending and descending favourable winds in the troposphere over the WTP in the El Niño minus La Niña and La Niña minus El Niño cases, respectively. Because the vertical variation of winds is considered to be the basic element driving convection over the region, we proceed to regress the vertical variations of winds averaged over 68° – 80°E onto the VTC over the MR. From Fig. 10, the impact of the MR VTC on the WTP is evident during ENSO years. In the El Niño minus La Niña case, the ascending winds (a sign of convection) are clearly seen in the upper vertical levels over the WTP, while in the La Niña minus El Niño case, descending winds (a sign of subsidence) are seen (Figs 10a and 10b). In other words, the composite analysis and causality analysis indicate that the VTC over the MR has a significant effect on WTP convection, which can induce ascending (descending) winds over the WTP between the 250 and 100 hPa levels during El Niño (La Niña) years. Based on these analyses, we can say that the MR VTC is closely related to the WTP, modulating the upper tropospheric variation and, hence, the large-scale circulation pattern over the WTP regions, thereby influencing the convection over the WTP.

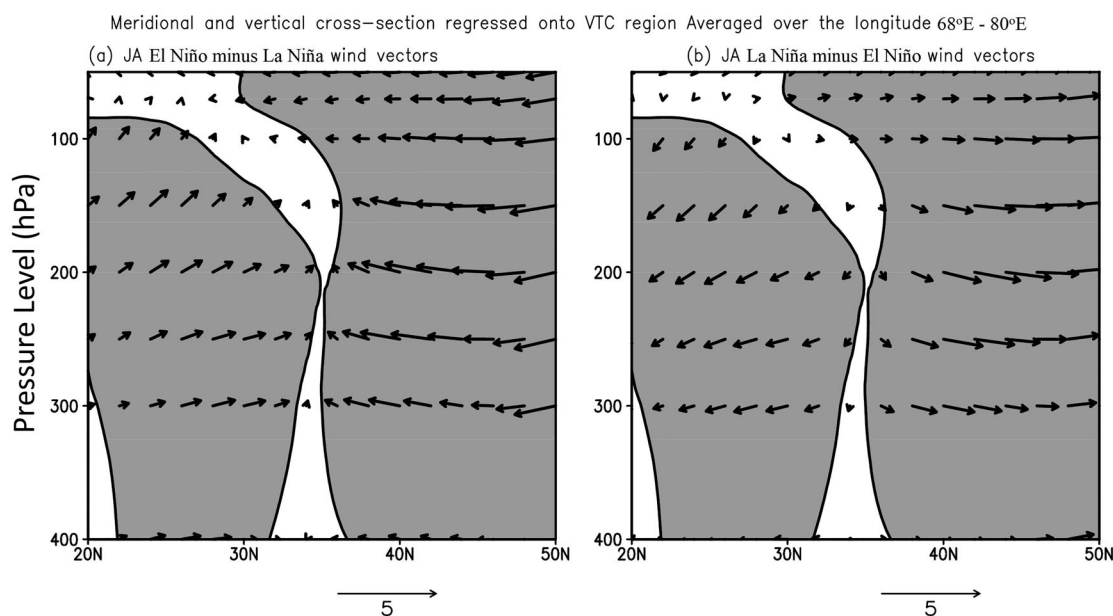


Fig. 10 Meridional and vertical cross-section distribution of the wind vectors (arrows; m s^{-1}) averaged over (68° – 80°E) at different pressure levels regressed onto VTC for (a) El Niño minus La Niña events and (b) La Niña minus El Niño events. The regression coefficients are statistically significant (grey shading) at the 99% confidence level based on a Student's *t*-test.

Hence, we can say that the vertical motion over the WTP is indeed impacted by the vertical temperature dipole structure over the MR. Apart from this, further attention has been given to exploring the possible pathways (i.e., the teleconnections) through which the VTC over the MR may impact the dynamics over the WTP. For this, the interference of the VTC over the MR with the subtropical jets over the region was explored. Previously, the subtropical jets were often found to act as a bridge between Europe and Asia in the summer (e.g., Branstator, 2002; Li et al., 2008). However, the role of the MR in possible interactions with the subtropical jets has not been examined. To examine its role, we analyzed the 200 hPa zonal winds (a proxy for subtropical jets) during El Niño (Fig. 11a) and La Niña (Fig. 11b) events, and, interestingly, an explicit subtropical jet can be seen linking Europe and Asia during both events. Looking more closely at the differences (i.e., El Niño minus La Niña events, Fig. 11c), significant changes in the so-called subtropical jets linking Europe and Asia can be seen over the MR region. A detailed analysis of Fig. 11c shows westerly winds over the southern part of the MR region in association with easterly winds over the northern part; this distribution implies a cyclonic circulation centred over the MR, in accordance with the results shown in Fig. 4b, which is favourable for local convection and is evident in Fig. 5. Also, the role of the VTC on the WTP over the MR is clearly reflected in a regression map shown in Fig. 11d, with a conspicuous feature (i.e., an induced cyclonic circulation by the MR VTC over the WTP) in agreement with the findings presented in Fig. 9b. Nevertheless, it is too early to make a conclusive statement; we would like to carry out a detailed study using adequate atmospheric general circulation models in the near future.

4 Summary

The MR is surrounded by three continents: Africa, Asia, and Europe and is known as one of the regions of the world most vulnerable to climate change (Giorgi, 2006). The surface of the MR has been continuously warmed over the last several decades, especially during midsummer (Volosciuk et al., 2016). The impact of this warming has been documented in several previous studies on both widespread synoptic systems and human health concerns (Tolika et al., 2009), but most of these studies have been limited to lower level temperature variations, with very few considering the upper layer TT. Recently, it has been reported that the upper TT variation also plays a key role in affecting precipitation and large-scale circulation (Zuo et al., 2012); hence, in this study we explored the upper TT variation over the MR and its potential impacts in the region and its surrounding area.

Using the gridded NCEP/NCAR daily values of upper TT between the pressure levels 400 and 50 hPa for the 1982–2017 period, we showed that a VTC exists in the upper troposphere centred over the MR. Further study explored the possible relationship between the MR upper thermal conditions and the WTP convection during the midsummer monsoon season; we also explored the associated physical mechanisms. With a recently developed causality analysis, we showed that the MR VTC has a significant impact on convection over the WTP during El Niño and La Niña years. We also showed that the MR VTC influences WTP convection through modulating the upper TT variation and, hence, the large-scale circulation pattern over the WTP regions. During El Niño (La Niña) years, the VTC over the MR seems to be concomitant with the WTP, with a conspicuous circulation structure;

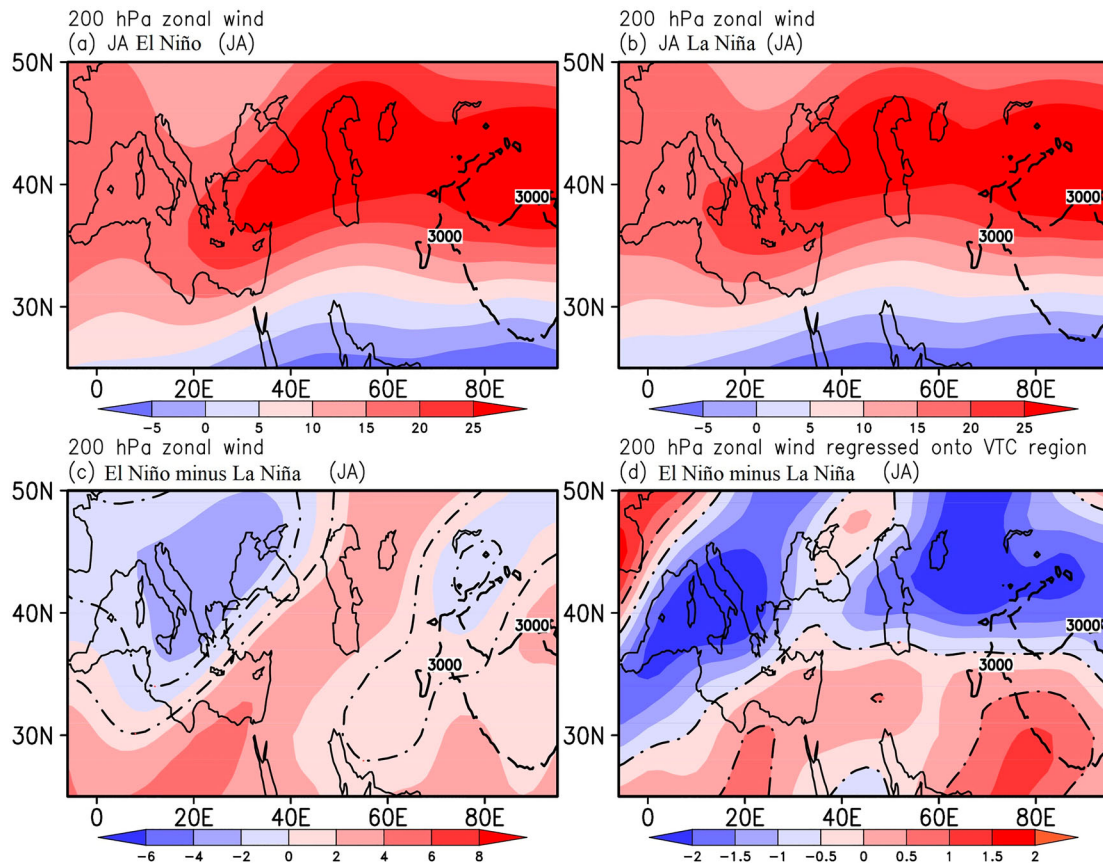


Fig. 11 JA zonal wind at 200 hPa (m s^{-1}) during (a) El Niño and (b) La Niña events. (c) is (a) minus (b), and (d) is the field shown in (c) regressed onto the VTC. The area enclosed by the thick black dot-dashed line is statistically significant at the 99% confidence level based on a Student's *t*-test. The dashed line marks the 3000 m topographic isoline.

correspondingly, the VTC over the MR induces ascending (descending) winds over the WTP between the 250 and 100 hPa levels during El Niño (La Niña) years. This finding of the upper tropospheric variation over the MR and, particularly, its effects on the WTP convection, to the best of our knowledge, has not been documented in the literature and has so far not received any attention. It is expected that this finding will help provide a fresh insight into the complex processes concomitant with the hydrology and geomorphology of the WTP.

Acknowledgements

We are grateful to the editor and three anonymous reviewers for their valuable comments and suggestions, which helped improve the manuscript in the present form. Thanks are due to the NCEP–DOE AMIP 2 Reanalysis, NOAA, and

MERRA teams for providing their respective datasets. The figures were prepared using GrADS.

Disclosure statement

No potential conflict of interest was reported by the author(s).

Funding

This research was supported by the National Science Foundation of China [grant number 41975064], the National Program on Global Change and Air-Sea Interaction [grant number GASI-IPOVAI-06], and the 2015 Jiangsu Program for Innovation Research and Entrepreneurship Groups.

ORCID

B. H. Vaid  <http://orcid.org/0000-0002-4572-1376>

References

Abe, M., Hori, M., Yasunari, T., & Kitoh, A. (2013). Effects of the Tibetan Plateau on the onset of the summer monsoon in South Asia: The role of the air-sea interaction. *Journal of Geophysical Research*, 118, 1760–1776. <https://doi.org/10.1002/jgrd.50210>

Abid, M. A., Kang, I. S., Almazroui, M., & Kucharski, F. (2015). Contribution of synoptic transients to the potential predictability of PNA circulation anomalies: El Niño versus La Niña. *Journal of Climate*, 28(21), 8347–8362. <https://doi.org/10.1175/JCLI-D-14-00497.1>

- Alpert, P., Abranski, R., & Neeman, B. U. (1990). The prevailing summer synoptic system in Israel-subtropical high, not Persian trough. *Israel Journal of Earth Sciences*, 39, 93–102.
- Alpert, P., Price, C., Krichak, S. O., Ziv, B., Saaroni, H., Osetinsky, I., Barkan, J., & Kishcha, P. (2005). Tropical tele-connections to the Mediterranean climate and weather. *Advances in Geosciences*, 2, 157–160. <https://doi.org/10.5194/adgeo-2-157-2005>
- Bao, Q., Yang, J., Liu, Y. M., Wu, G. X., & Wang, B. (2010). Roles of anomalous Tibetan Plateau warming on the severe 2008 winter storm in central-southern China. *Monthly Weather Review*, 138(6), 2375–2384. <https://doi.org/10.1175/2009MWR2950.1>
- Barry, R. G., & Chorley, R. J. (2003). *Atmosphere, weather, and climate* (8th ed). Routledge.
- Beniston, M., & Stephenson, D. B. (2004). Extreme climatic events and their evolution under changing climatic conditions. *Global and Planetary Change*, 44(1-4), 1–9. <https://doi.org/10.1016/j.gloplacha.2004.06.001>
- Bjerknes, J. (1969). Atmospheric teleconnections from the equatorial Pacific. *Monthly Weather Review*, 97(3), 163–172. [https://doi.org/10.1175/1520-0493\(1969\)097<0163:ATFTEP>2.3.CO;2](https://doi.org/10.1175/1520-0493(1969)097<0163:ATFTEP>2.3.CO;2)
- Branstator, G. (2002). Circumglobal teleconnections, the jet stream waveguide, and the North Atlantic Oscillation. *Journal of Climate*, 15(14), 1893–1910. [https://doi.org/10.1175/1520-0442\(2002\)015<1893:CTTJSW>2.0.CO;2](https://doi.org/10.1175/1520-0442(2002)015<1893:CTTJSW>2.0.CO;2)
- Bronnimann, S. (2007). Impact of El Niño-Southern oscillation on European climate. *Reviews of Geophysics*, 45(RG3003), 1–28. <https://doi.org/10.1029/2006RG000199>
- Brunetti, M., Buffoni, L., Mangianti, F., Maugeri, M., & Nanni, T. (2004). Temperature, precipitation and extreme events during the last century in Italy. *Global and Planetary Change*, 40(1-2), 141–149. [https://doi.org/10.1016/S0921-8181\(03\)00104-8](https://doi.org/10.1016/S0921-8181(03)00104-8)
- Chiodi, A. M., & Harrison, D. E. (2015). Equatorial Pacific easterly wind surges and the onset of La Niña events. *Journal of Climate*, 28(2), 776–792. <https://doi.org/10.1175/JCLI-D-14-00227.1>
- Ciric, D., Nieto, R., Losada, L., Drumond, A., & Gimeno, L. (2018). The Mediterranean moisture contribution to climatological and extreme monthly continental precipitation. *Water*, 10(4), 519. <https://doi.org/10.3390/w10040519>
- Ehsan, M. A., Kang, I. S., Almazroui, M., Abid, M. A., & Kucharski, F. (2013). A quantitative assessment of changes in seasonal potential predictability for the twentieth century. *Climate Dynamics*, 41(9-10), 9–10. <https://doi.org/10.1007/s00382-013-1874-x>
- Fekete, B. M., Vorosmarty, C. J., & Grabs, W. (1999). *Global, composite runoff fields based on observed river discharge and simulated water balances* (Technical Report No. 22, pp. 1–109). Global Runoff Data Center. https://www.bafg.de/GRDC/EN/02_srvcs/24_rprt/rs/report_22.pdf?__blob=publicationFile
- Fekete, B. M., Vorosmarty, C. J., & Grabs, W. (2000). *UNH/GRDC composite runoff fields V 1.0*. Complex Systems Research Center, University of New Hampshire and Koblenz, Germany: Global Runoff Data Center (GRDC). <http://www.grdc.sr.unh.edu/>
- Giorgi, F. (2006). Climate change hot-spots. *Geophysical Research Letters*, 33(8), L08707. <https://doi.org/10.1029/2006GL025734>
- Immerzeel, W. W., VanBeek, L. P. H., & Bierkens, M. F. P. (2010). Climate change will affect the Asian water towers. *Science*, 328(5984), 1382–1385. <https://doi.org/10.1126/science.1183188>
- Kanamitsu, M., Ebisuzaki, W., Woollen, J., Yang, S. K., Hnilo, J. J., Fiorino, M., & Potter, G. L. (2002). NCEP-DOE AMIP-II reanalysis (R-2). *Bulletin of the American Meteorological Society*, 83(11), 1631–1643. <https://doi.org/10.1175/BAMS-83-11-1631>
- Kessler, W. S. (2002). Is ENSO a cycle or a series of events? *Geophysical Research Letters*, 29(23), 2125. <https://doi.org/10.1029/2002GL015924>
- Kitoh, A. (2004). Effects of mountain uplift on East Asian summer climate investigated by a coupled atmosphere-ocean GCM. *Journal of Climate*, 17(4), 783–802. [https://doi.org/10.1175/1520-0442\(2004\)017<0783:EOMUOE>2.0.CO;2](https://doi.org/10.1175/1520-0442(2004)017<0783:EOMUOE>2.0.CO;2)
- Li, G., Ren, B. H., Yang, C. Y., & Zheng, J. Q. (2010). Indices of El Niño and El Niño Modoki: An improved El Niño Modoki index. *Advances in Atmospheric Sciences*, 27(5), 1210–1220. <https://doi.org/10.1007/s00376-010-9173-5>
- Li, J., Yu, R., & Zhou, T. (2008). Teleconnection between NAO and climate downstream of the Tibetan Plateau. *Journal of Climate*, 21(18), 4680–4690. <https://doi.org/10.1175/2008JCLI2053.1>
- Liang, X. S. (2014). Unraveling the cause-effect relation between time series. *Physical Review E*, 90(5), 1–11. <https://doi.org/10.1103/PhysRevE.90.052150>
- Liang, X. S. (2015). Normalizing the causality between time series. *Physical Review E*, 92(2), 1–6. <https://doi.org/10.1103/PhysRevE.92.022126>
- Liang, X. S. (2016). Information flow and causality as rigorous notions ab initio. *Physical Review E*, 94(5), 1–28. <https://doi.org/10.1103/PhysRevE.94.052201>
- Liang, X. S. (2018). Causation and information flow with respect to relative entropy. *Chaos: An Interdisciplinary Journal of Nonlinear Science*, 28(7), 1–9. <https://doi.org/10.1063/1.5010253>
- Lin, P., Wei, J., Yang, Z. L., Zhang, Y., & Zhang, K. (2016). Snow data assimilation-constrained land initialization improves seasonal temperature prediction. *Geophysical Research Letters*, 43(21), 11,423–11,432. <https://doi.org/10.1002/2016GL070966>
- Lionello, P., Malanotte-Rizzoli, P., Boscolo, R., Alpert, P., Artale, V., Li, L., Luterbacher, J., May, W., Trigo, R., Tsimplis, M., Ulbrich, U., & Xoplaki, E. (2006). The Mediterranean climate: An overview of the main characteristics and issues. *Development of Earth Environmental Sciences*, 4, 1–26. [https://doi.org/10.1016/S1571-9197\(06\)80003-0](https://doi.org/10.1016/S1571-9197(06)80003-0)
- Liu, X. D., & Yanai, M. (2001). Relationship between the Indian monsoon precipitation and the tropospheric temperature over the Eurasian continent. *Quarterly Journal of the Royal Meteorological Society*, 127(573), 909–937. <https://doi.org/10.1002/qj.49712757311>
- Ma, Y., Ma, W., Zhong, L., Hu, Z., Li, M., Zhu, Z., Han, C., Wang, B., & Liu, X. (2017). Monitoring and modeling the Tibetan Plateau's climate system and its impact on East Asia. *Scientific Reports*, 7(1), 44574. <https://doi.org/10.1038/srep44574>
- Mathieu, P. P., Sutton, R. T., Dong, B. W., & Collins, M. (2004). Predictability of winter climate over the North Atlantic European region during ENSO events. *Journal of Climate*, 17(10), 1953–1974. [https://doi.org/10.1175/1520-0442\(2004\)017<1953:POWCOT>2.0.CO;2](https://doi.org/10.1175/1520-0442(2004)017<1953:POWCOT>2.0.CO;2)
- Meteorological Office. (1962). *Weather in the Mediterranean* (Pub. 391, Vol. 1). HMSO.
- NOAA. (2019a). NCEP-DOE reanalysis 2: Summary. <https://www.esrl.noaa.gov/psd/data/gridded/data.ncep.reanalysis2.html>
- NOAA. (2019b). NOAA optimum interpolation (OI) sea surface temperature (SST) V2. <https://www.esrl.noaa.gov/psd/data/gridded/data.noaa.oisst.v2.html>
- Orsolini, Y. J., Senan, R., Balsamo, G., Doblas-Reyes, F. J., Vitart, F., Weisheimer, A., Carrasco, A., & Benestad, R. E. (2013). Impact of snow initialization on sub-seasonal forecasts. *Climate Dynamics*, 41(7-8), 1969–1982. <https://doi.org/10.1007/s00382-013-1782-0>
- Reynolds, R. W., Rayner, N. A., Smith, T. M., Stokes, D. C., & Wang, W. (2002). An improved in situ and satellite SST analysis for climate. *Journal of Climate*, 15(13), 1609–1625. [https://doi.org/10.1175/1520-0442\(2002\)015<1609:AIISAS>2.0.CO;2](https://doi.org/10.1175/1520-0442(2002)015<1609:AIISAS>2.0.CO;2)
- Rienecker, M. M., Suarez, M. J., Gelaro, R., Todling, R., Bacmeister, J., Liu, E., Bosilovich, M. G., Schubert, S. D., Takacs, L., Kim, G.-K., Bloom, S., Chen, J., Collins, D., Conaty, A., da Silva, A., Gu, W., Joiner, J., Koster, R. D., Lucchesi, R., ... Woollen, J. (2011). MERRA: NASA's modern-era retrospective analysis for research and applications. *Journal of Climate*, 24(14), 3624–3648. <https://doi.org/10.1175/JCLI-D-11-00015.1>
- Ropelewski, C. F., & Halpert, M. S. (1987). Global and regional scale precipitation patterns associated with the El Niño/Southern Oscillation (ENSO). *Monthly Weather Review*, 115(8), 1606–1626. [https://doi.org/10.1175/1520-0493\(1987\)115<1606:GARSPP>2.0.CO;2](https://doi.org/10.1175/1520-0493(1987)115<1606:GARSPP>2.0.CO;2)
- Saaroni, H., & Ziv, B. (2000). Summer rainfall in a Mediterranean climate-The case of Israel: Climatological-dynamical analysis. *International Journal of Climatology*, 20(2), 191–209. [https://doi.org/10.1002/\(SICI\)1097-0088\(200002\)20:2<191::AID-JOC464>3.0.CO;2-E](https://doi.org/10.1002/(SICI)1097-0088(200002)20:2<191::AID-JOC464>3.0.CO;2-E)
- Saaroni, H., Ziv, B., Edelson, J., & Alpert, P. (2003). Longterm variations in summer temperatures over the Eastern mediterranean. *Geophysical Research Letters*, 30(18), 1946. <https://doi.org/10.1029/2003GL017742>

- Senan, R., Orsolini, Y. J., Weisheimer, A., Vitart, F., Balsamo, G., Stockdale, T., Dutra, E., Doblas-Reyes, F. J., & Basang, D. (2016). Impact of spring-time Himalayan-Tibetan Plateau snowpack on the onset of the Indian summer monsoon in coupled seasonal forecasts. *Climate Dynamics*, 47(9-10), 2709–2725. <https://doi.org/10.1007/s00382-016-2993-y>
- Seneviratne, S. I., Donat, M. G., Pitman, A. J., Knutti, R., & Wilby, R. L. (2016). Allowable CO₂ emissions based on regional and impact-related climate targets. *Nature*, 529(7587), 477–483. <https://doi.org/10.1038/nature16542>
- Sodemann, H., & Zuber, E. (2010). Seasonal and inter-annual variability of the moisture sources for alpine precipitation during 1995-2002. *International Journal of Climatology*, 30, 947–961. <https://doi.org/10.1002/joc.1932>
- Stocker, T. F., Qin, D., Plattner, G.-K., Tignor, M., Allen, S. K., Boschung, J., Nauels, A., Xia, Y., Bex, V., & Midgley, P. M. (Eds.). (2013). *Climate change 2013: The physical science basis. Contribution of Working Group I to the Fifth Assessment Report of the Intergovernmental Panel on climate change*. Cambridge University Press.
- Tolika, K., Maheras, P., & Tegoulis, I. (2009). Extreme temperatures in Greece during 2007: Could this be a “return to the future”? *Geophysical Research Letters*, 36(10), L10813. <https://doi.org/10.1029/2009GL038538>
- Vaid, B. H., & Liang, X. S. (2015). Tropospheric temperature gradient and its relation to the South and East Asian precipitation variability. *Meteorological and Atmospheric Physics*, 127(3), 579–585. <https://doi.org/10.1007/s00703-015-0385-1>
- Vaid, B. H., & Liang, X. S. (2018a). The changing relationship between the convection over the western Tibetan Plateau and the sea surface temperature in the northern Bay of Bengal. *Tellus A: Dynamic Meteorology and Oceanography*, 70(1), 1440869. <https://doi.org/10.1080/16000870.2018.1440869>
- Vaid, B. H., & Liang, X. S. (2018b). An abrupt change in tropospheric temperature gradient and moisture transport over East Asia in the late 1990s. *Atmosphere-Ocean*, 56(4), 268–276. <https://doi.org/10.1080/07055900.2018.1429381>
- Vaid, B. H., & Liang, X. S. (2019). Influence of tropospheric temperature gradient on the boreal wintertime precipitation over East Asia. *Terrestrial, Atmospheric and Oceanic Sciences*, 30(2), 1–10. <https://doi.org/10.3319/TAO.2018.10.24.01>
- Volosciuk, C., Maraun, D., Semenov, V. A., Tilinina, N., Gulev, S. K., & Latif, M. (2016). Rising Mediterranean sea surface temperatures amplify extreme summer precipitation in central Europe. *Scientific Reports*, 6(1), 32450. <https://doi.org/10.1038/srep32450>
- Wang, B., Bao, Q., Hoskins, B., Wu, G. X., & Liu, Y. M. (2008). Tibetan Plateau warming and precipitation changes in East Asia. *Geophysical Research Letters*, 35(14), L14702. <https://doi.org/10.1029/2008GL034330>
- Ward, P. J., Eisner, S., Flörke, M., Dettinger, M. D., & Kummerow, M. (2014). Annual flood sensitivities to ENSO at the global scale. *Hydrological Earth System Sciences*, 18(1), 47–66. <https://doi.org/10.5194/hess-18-47-2014>
- Wu, G. X., Duan, A. M., Liu, Y. M., Mao, J. Y., Ren, R. C., Bao, Q., He, B., Liu, B. Q., & Hu, W. T. (2015). Tibetan Plateau climate dynamics: Recent research progress and outlook. *National Science Review*, 2(1), 100–116. <https://doi.org/10.1093/nsr/nwu045>
- Wu, G. X., Liu, Y. M., He, B., Bao, Q., Duan, A. M., & Jin, F. F. (2012b). Thermal controls on the Asian summer monsoon. *Scientific Reports*, 2(404), 1–7. doi:10.1038/srep00404
- Wu, Z. W., Li, J. P., Jiang, Z. H., & Ma, T. T. (2012a). Modulation of the Tibetan plateau snow cover on the ENSO teleconnections: From the East Asian summer monsoon perspective. *Journal of Climate*, 25(7), 2481–2489. <https://doi.org/10.1175/JCLI-D-11-00135.1>
- Wu, Z., Zhang, P., Chen, H., & Li, Y. (2016). Can the Tibetan Plateau snow cover influence the interannual variations of Eurasian heat wave frequency? *Climate Dynamics*, 46(11-12), 3405–3417. <https://doi.org/10.1007/s00382-015-2775-y>
- Xoplaki, E., González-Rouco, F., Luterbacher, J., & Wanner, H. (2004). Wet season Mediterranean precipitation variability: Influence of large-scale dynamics and trends. *Climate Dynamics*, 23(1), 63–78. <https://doi.org/10.1007/s00382-004-0422-0>
- Xu, X., Lu, C., Shi, X., & Gao, S. (2008). World water tower: An atmospheric perspective. *Geophysical Research Letters*, 35(20), 525–530. <https://doi.org/10.1029/2008GL035867>
- Ye, T. Z., & Gao, Y. X. (1979). *The meteorology of the Qinghai-Xizang (Tibet) Plateau*. Science Press.
- Yu, J. Y., & Zou, Y. (2013). The enhanced drying effect of central-Pacific El Niño on U.S. winter. *Environmental Research Letters*, 8(1), 014019. <https://doi.org/10.1088/1748-9326/8/1/014019>
- Zhou, B. T., & Zhao, P. (2010). Influence of the Asian-Pacific oscillation on spring precipitation over central eastern China. *Advances in Atmospheric Sciences*, 27(3), 575–582. <https://doi.org/10.1007/s00376-009-9058-7>
- Zuo, Z. Y., Yang, S., Kumar, A., Zhang, R. H., Xue, Y., & Jha, B. (2012). Role of thermal conditions over Asia in the weakening Asian summer monsoon under global warming background. *Journal of Climate*, 25(9), 3431–3436. <https://doi.org/10.1175/JCLI-D-11-00742.1>